

Chapter 2

Transfer Matrix Method and the Graded-Index Waveguide

Abstract The transfer matrix method used in thin-film optics is extremely useful when applied to analyze the propagation characteristics of electromagnetic waves in planar multilayer optical waveguides. This chapter aims to extend the transfer matrix method to treat the bound modes of the graded-index waveguide. Beginning with a brief introduction of the transfer matrix, we derived the eigenvalue equations and studied the multilayer optical waveguides. Different from the widely used WKB approximation, the transfer matrix obtained some important but different conclusions when applied to the graded-index waveguide, such as the exact phase shift at the classical turning points.

Keywords Transfer matrix method · Eigenvalue equation · WKB approximation · Graded-index waveguide

2.1 The Transfer Matrix and Its Characteristics

The 2×2 transfer matrix is a fruitful tool widely applied in optics to treat layered systems, such as superlattices or multilayered waveguide. And it is receiving more and more attention for its advantages such as easy computing and high accuracy. For example, it was used by M. Born and E. Wolf to investigate the transmission and reflection characteristics of light propagation through multilayer structures [1]. When dealing with multi-lens optical device or media, at each interface, the light is partially transmitted and partially reflected, and the matrix method can also provide good results [2]. In this section, we use some special solutions of the wave equation to construct a transfer matrix, which is a real matrix with clear physical insight. And in the rest of this chapter, the reader may find this method approachable and intriguing.

In optics, the regions with variable refractive index are usually approximated as a series of steps at a group of points, and between two adjacent points, the refractive index is treated as constant. So the polarization transfer matrix of the TE and TM

mode can be derived from the one-dimensional scalar wave equation to characterize the optical properties of these thin segments.

Considering the refractive index profile $n(x)$ of arbitrary shape as plotted in Fig. 2.1, without loss of generality, and we divide the region between the points of $x = a$ and $x = b$ into l subregions, and the width of each subregion is given by

$$w_j = x_j - x_{j-1} \quad (j = 1, 2, \dots, l), \quad (2.1)$$

which becomes smaller with increasing l . In that case, the refractive index in the subregion can be viewed as homogeneous, and its strength is given by

$$n_j = n\left(\frac{x_{j-1} + x_j}{2}\right) \quad (j = 1, 2, \dots, l). \quad (2.2)$$

Take the TE mode, for example, and let $\psi_j(x)$ denotes any field component of the electromagnetic distribution in the j th subregion (x_{j-1}, x_j) , which satisfies the following scalar wave equation

$$\frac{d^2\psi_j(x)}{dx^2} + \kappa_j^2(x)\psi_j(x) = 0 \quad (j = 1, 2, \dots, l), \quad (2.3)$$

with $\kappa_j^2(x) = k_0^2 n_j^2 - \beta^2$. Here, β is the propagation constant and κ_j denotes the wave number. At the interface $x = x_{j-1}$ between the $(j-1)$ th and j th subregions, the continuity conditions of the wave function requires that

$$\begin{bmatrix} \psi_j(x_{j-1}) \\ \psi'_j(x_{j-1}) \end{bmatrix} = \begin{bmatrix} \psi_{j-1}(x_{j-1}) \\ \psi'_{j-1}(x_{j-1}) \end{bmatrix}. \quad (2.4)$$

Solving Eq. (2.3), the wave function in the j th subregion has the following form

$$\begin{cases} \psi_j(x) = A_j e^{i\kappa_j x} + B_j e^{-i\kappa_j x} \\ \psi'_j(x) = i\kappa_j (A_j e^{i\kappa_j x} - B_j e^{-i\kappa_j x}) \end{cases}, \quad (2.5)$$

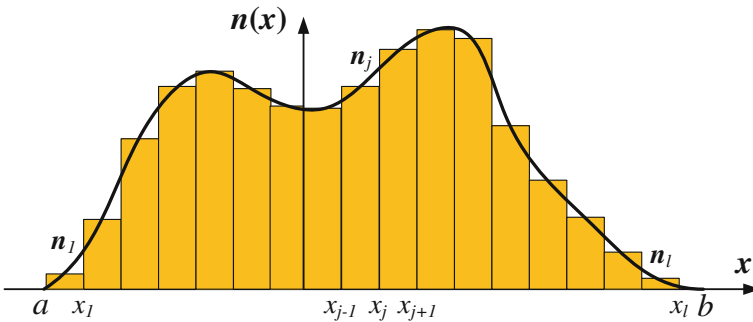


Fig. 2.1 One-dimensional refractive index profile of arbitrary distribution

which can be recast into a matrix form

$$\begin{bmatrix} \psi_j(x) \\ \psi'_j(x) \end{bmatrix} = \begin{bmatrix} e^{i\kappa_j x} & e^{-i\kappa_j x} \\ i\kappa_j e^{i\kappa_j x} & -i\kappa_j e^{-i\kappa_j x} \end{bmatrix} \begin{bmatrix} A_j \\ B_j \end{bmatrix}. \quad (2.6)$$

So at the point $x = x_j$, there is

$$\begin{bmatrix} \psi_j(x_j) \\ \psi'_j(x_j) \end{bmatrix} = \begin{bmatrix} e^{i\kappa_j x_j} & e^{-i\kappa_j x_j} \\ i\kappa_j e^{i\kappa_j x_j} & -i\kappa_j e^{-i\kappa_j x_j} \end{bmatrix} \begin{bmatrix} A_j \\ B_j \end{bmatrix}, \quad (2.7)$$

and at $x = x_{j-1}$, we can write down a similar matrix equation as follows:

$$\begin{bmatrix} \psi_j(x_{j-1}) \\ \psi'_j(x_{j-1}) \end{bmatrix} = \begin{bmatrix} e^{i\kappa_j x_{j-1}} & e^{-i\kappa_j x_{j-1}} \\ i\kappa_j e^{i\kappa_j x_{j-1}} & -i\kappa_j e^{-i\kappa_j x_{j-1}} \end{bmatrix} \begin{bmatrix} A_j \\ B_j \end{bmatrix}. \quad (2.8)$$

Combining Eqs. (2.7) and (2.8) yields

$$\begin{bmatrix} \psi_j(x_j) \\ \psi'_j(x_j) \end{bmatrix} = \begin{bmatrix} e^{i\kappa_j x_j} & e^{-i\kappa_j x_j} \\ i\kappa_j e^{i\kappa_j x_j} & -i\kappa_j e^{-i\kappa_j x_j} \end{bmatrix} \begin{bmatrix} e^{i\kappa_j x_{j-1}} & e^{-i\kappa_j x_{j-1}} \\ i\kappa_j e^{i\kappa_j x_{j-1}} & -i\kappa_j e^{-i\kappa_j x_{j-1}} \end{bmatrix}^{-1} \begin{bmatrix} \psi_j(x_{j-1}) \\ \psi'_j(x_{j-1}) \end{bmatrix}. \quad (2.9)$$

Through some basic matrix operations, Eq. (2.9) becomes

$$\begin{bmatrix} \psi_j(x_j) \\ \psi'_j(x_j) \end{bmatrix} = M_j \begin{bmatrix} \psi_j(x_{j-1}) \\ \psi'_j(x_{j-1}) \end{bmatrix}, \quad (2.10)$$

where

$$M_j = \begin{bmatrix} \cos(\kappa_j w_j) & \frac{1}{\kappa_j} \sin(\kappa_j w_j) \\ -\kappa_j \sin(\kappa_j w_j) & \cos(\kappa_j w_j) \end{bmatrix} \quad (j = 1, 2, \dots, l). \quad (2.11)$$

and $w_j = x_j - x_{j-1}$ is the width of the subregion. Equation (2.11) is known as the transfer matrix in the subregion (x_{j-1}, x_j) , which connects the wave function and its first derivative at the two boundaries of the j th subregion. And according to the boundary condition Eq. (2.4), the wave function and derivative at the boundary of the j th subregion are further connected with those at the $(j-1)$ th subregion's boundary by

$$\begin{bmatrix} \psi_j(x_j) \\ \psi'_j(x_j) \end{bmatrix} = M_j \begin{bmatrix} \psi_{j-1}(x_{j-1}) \\ \psi'_{j-1}(x_{j-1}) \end{bmatrix}. \quad (2.12)$$

Take the TM mode into consideration, and the more generalized transfer matrix has the following form

$$M(w) = \begin{bmatrix} \cos(\kappa w) & \frac{f}{\kappa} \sin(\kappa w) \\ -\frac{\kappa}{f} \sin(\kappa w) & \cos(\kappa w) \end{bmatrix}, \quad (2.13)$$

where

$$f = \begin{cases} 1, & (TE) \\ n^2 & (TM) \end{cases}. \quad (2.14)$$

Before embarking on complicated issues, it is necessary to provide some discussion on the basic characteristics of the transfer matrix. For convenience, the 2×2 transfer matrix is rewritten as follows:

$$M = \begin{bmatrix} m_{11} & m_{12} \\ m_{21} & m_{22} \end{bmatrix}.$$

- (a) Combining Eqs. (2.13) and (2.14), it is easy to found that in a non-absorptive medium, the matrix is a unimodular matrix with real coefficient

$$\det(M) = \begin{vmatrix} m_{11} & m_{12} \\ m_{21} & m_{22} \end{vmatrix} = m_{11}m_{22} - m_{12}m_{21} = 1, \quad (2.15)$$

where “det” represents a determinant. The physical insight of Eq. (2.15) is the conservation of energy.

- (b) The energy eigenvalues λ of the transfer matrix can be determined via the secular equation

$$|M - \lambda I| = 0, \quad (2.16)$$

where I denotes the units matrix. Solving Eq. (2.16), and note that the modulus of the matrix equals unit, one can obtain the following equation:

$$\lambda^2 - (m_{11} + m_{22})\lambda + 1 = 0. \quad (2.17)$$

Equation (2.17) shows that the two eigenvalues of the matrix λ_1 and λ_2 are reciprocal to each other. Generally, the two eigenvalue can be expressed as follows:

$$\begin{cases} \lambda_1 = e^{i\kappa w} \\ \lambda_2 = e^{-i\kappa w} \end{cases}, \quad (2.18)$$

where the physics behind κ and h is determined by the specific structure. And according to Eq. (2.17), apparently there is

$$\cos(\kappa w) = \frac{1}{2}(m_{11} + m_{22}) = \frac{1}{2}\text{Tr}M(w), \quad (2.19)$$

where “Tr” denotes the trace of the matrix. Equation (2.19) is an important formula for studying periodic structures, which is intimately connected with the Bloch theorem.

- (c) Consider a stepped double potential well, and let $M(w_1)$ and $M(w_2)$ be the transfer matrix of the two adjacent homogeneous wells, respectively. According to Eq. (2.12), we have

$$\begin{bmatrix} \psi(w_1) \\ \psi'(w_1) \end{bmatrix} = M(w_1) \begin{bmatrix} \psi(0) \\ \psi'(0) \end{bmatrix} \quad (2.20)$$

and

$$\begin{bmatrix} \psi(w_1 + w_2) \\ \psi'(w_1 + w_2) \end{bmatrix} = M(w_2) \begin{bmatrix} \psi(w_1) \\ \psi'(w_1) \end{bmatrix}. \quad (2.21)$$

So there is

$$\begin{bmatrix} \psi(w_1 + w_2) \\ \psi'(w_1 + w_2) \end{bmatrix} = M(w_1 + w_2) \begin{bmatrix} \psi(0) \\ \psi'(0) \end{bmatrix}, \quad (2.22)$$

where

$$M(w_1 + w_2) = M(w_2)M(w_1). \quad (2.23)$$

Note that $M(w_2)$ and $M(w_1)$ in Eq. (2.23) cannot be swapped. The above consequent can be extended immediately to multilayer structure. Assume the respective width of a N -layer structure is w_1, w_2, \dots, w_N , the corresponding matrixes of these homogeneous layers are $M(w_1), M(w_2), \dots, M(w_N)$, and the transfer matrix of the whole structure is

$$M(w_1 + w_2 + \dots + w_N) = M(w_N)M(w_{N-1}) \cdots M(w_2)M(w_1). \quad (2.24)$$

- (d) Periodic refractive index distribution, i.e., one-dimensional photonic crystal is common but extremely important. If the lattice length is Λ , and the transfer matrix for a single cell is

$$M(\Lambda) = \begin{bmatrix} m_{11} & m_{12} \\ m_{21} & m_{22} \end{bmatrix}, \quad (2.25)$$

then we can write down the transfer matrix for the whole lattice as

$$M(N\Lambda) = \underbrace{M(\Lambda) \cdot M(\Lambda) \cdots M(\Lambda)}_{N \text{ times}} = [M(\Lambda)]^N. \quad (2.26)$$

It is easy to prove from the above formula

$$[M(\Lambda)]^N = U_{N-1}(\chi)M(\Lambda) - U_{N-2}(\chi)E, \quad (2.27)$$

where $U_N(\chi)$ denotes the second-class Chebyshev polynomial

$$U_N(\chi) = \frac{\sin[(N+1)\arccos\chi]}{\sqrt{1-\chi^2}}. \quad (2.28)$$

Equation (2.26) can also be written as follows:

$$\begin{aligned} M(N\Lambda) &= [M(\Lambda)]^N \\ &= U_{N-1}(\chi) \begin{bmatrix} m_{11} & m_{12} \\ m_{21} & m_{22} \end{bmatrix} - U_{N-2}(\chi) \begin{bmatrix} 1 & 0 \\ 0 & 1 \end{bmatrix} \\ &= \begin{bmatrix} m_{11}U_{N-1}(\chi) - U_{N-2}(\chi) & m_{12}U_{N-1}(\chi) \\ m_{21}U_{N-1}(\chi) & m_{22}U_{N-1}(\chi) - U_{N-2}(\chi) \end{bmatrix}. \end{aligned} \quad (2.29)$$

By setting

$$M(\Lambda) = \begin{bmatrix} \cos \kappa \Lambda & \frac{f}{\kappa} \sin \kappa \Lambda \\ -\frac{\kappa}{f} \sin \kappa \Lambda & \cos \kappa \Lambda \end{bmatrix}, \quad (2.30)$$

we can recast Eq. (2.29) into

$$M(N\Lambda) = \begin{bmatrix} \cos(N\kappa\Lambda) & \frac{f}{\kappa} \sin(N\kappa\Lambda) \\ -\frac{\kappa}{f} \sin(N\kappa\Lambda) & \cos(N\kappa\Lambda) \end{bmatrix}. \quad (2.31)$$

(e) The inverse of the transfer matrix is defined by

$$MM^{-1} = I, \quad (2.32)$$

and for the transfer matrix, it is easy to find

$$M^{-1} = \begin{bmatrix} m_{22} & -m_{12} \\ -m_{21} & m_{11} \end{bmatrix}. \quad (2.33)$$

Using the inverse matrix, one can obtain the reverse transfer relationship. By multiplying $M^{-1}(h)$ on both sides of Eq. (2.12) yields

$$\begin{bmatrix} \psi_{j-1}(x_{j-1}) \\ \psi'_{j-1}(x_{j-1}) \end{bmatrix} = \begin{bmatrix} \cos(\kappa_j h_j) & -\frac{1}{\kappa_j} \sin(\kappa_j h_j) \\ \kappa_j \sin(\kappa_j h_j) & \cos(\kappa_j h_j) \end{bmatrix} \begin{bmatrix} \psi_j(x_j) \\ \psi'_j(x_j) \end{bmatrix}. \quad (2.34)$$

Since both the transfer matrix and its inverse can relate the wave function at two points, they are both referred as transfer matrix in the rest of the book, while the only difference is the different transfer direction.

- (f) If we have $k_0^2 n^2 < \beta^2$ in a thin layer, then the solution of the scalar wave equation in this region is the superposition of two exponential functions, while the transverse wave number κ corresponding to oscillating field is replaced by an attenuation coefficient α , and there is

$$\kappa = i\alpha. \quad (2.35)$$

Note that

$$\begin{cases} \sin(ix) = i \sinh(x) \\ \cos(ix) = \cosh(x) \end{cases}, \quad (2.36)$$

Equation (2.13) should also be replaced by the following expression

$$M_j = \begin{bmatrix} \cosh(\alpha_j h_j) & \frac{1}{\alpha_j} \sinh(\alpha_j h_j) \\ \alpha_j \sinh(\alpha_j h_j) & \cosh(\alpha_j h_j) \end{bmatrix}, \quad (2.37)$$

while its inverse is

$$M_j^{-1} = \begin{bmatrix} \cosh(\alpha_j h_j) & -\frac{1}{\alpha_j} \sinh(\alpha_j h_j) \\ -\alpha_j \sinh(\alpha_j h_j) & \cosh(\alpha_j h_j) \end{bmatrix}. \quad (2.38)$$

2.2 The Eigenvalue Equation

Consider a simple planar waveguide, whose refractive index distribution is plotted in Fig. 2.2, and this section is aimed to calculate its eigenvalue spectrum. Since the transfer matrix, which connects the wave function and its first derivative at the two interfaces of a thin layer, represents the characteristic parameters of the dielectric slab, the field distribution in the guiding layer is not need to be considered. As a result, this procedure will be much simplified if the transfer matrix is applied, we only need to determine the wave function in the regions of $x < 0$ and $x > w$.

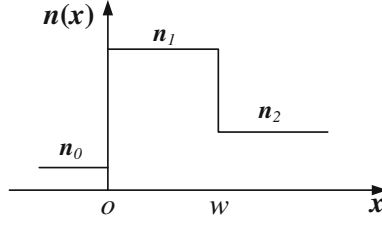


Fig. 2.2 Refractive index distribution of a planar waveguide with three dielectric layers

For the refractive index as plotted in Fig. 2.2, the transverse component of the TE mode transmitted in the guiding layer between the dielectric layer of n_0 and n_2 is as follows:

$$E_y(x) = \begin{cases} A \exp(p_0 x) & -\infty < x < 0 \\ D \exp[-p_2(x - w)] & w < x < +\infty \end{cases}, \quad (2.39)$$

and it follows

$$\begin{cases} E_y(0) = A \\ E'_y(0) = p_0 A \\ E_y(h) = D \\ E'_y(h) = -p_2 D \end{cases}. \quad (2.40)$$

Substituting the above equation into Eq. (2.12), one obtains

$$A \begin{bmatrix} 1 \\ p_0 \end{bmatrix} = \begin{bmatrix} \cos(\kappa_1 h) & -\frac{1}{\kappa_1} \sin(\kappa_1 h) \\ \kappa_1 \sin(\kappa_1 h) & \cos(\kappa_1 h) \end{bmatrix} \begin{bmatrix} 1 \\ -p_2 \end{bmatrix} D. \quad (2.41)$$

Multiply both sides of the above equation by a row vector $[-p_0 \ 1]$, there is

$$[-p_0 \ 1] \begin{bmatrix} \cos(\kappa_1 h) & -\frac{1}{\kappa_1} \sin(\kappa_1 h) \\ \kappa_1 \sin(\kappa_1 h) & \cos(\kappa_1 h) \end{bmatrix} \begin{bmatrix} 1 \\ -p_2 \end{bmatrix} = 0, \quad (2.42)$$

and by solving the above equation, it yields

$$\tan(\kappa_1 h) = \frac{p_0 + p_2}{\kappa_1 \left(1 - \frac{p_0 p_2}{\kappa_1^2}\right)}. \quad (2.43)$$

Eq. (2.43) can be called as the mode eigenvalue equation of TE polarization. If we take the boundary condition of the TM mode into consideration, the mode eigenvalue equation for TM mode can be written as follows:

$$\begin{bmatrix} -\frac{p_0}{n_0^2} & 1 \end{bmatrix} \begin{bmatrix} \cos(\kappa_1 h) & -\frac{n_1^2}{\kappa_1} \sin(\kappa_1 h) \\ \frac{\kappa_1}{n_1^2} \sin(\kappa_1 h) & \cos(\kappa_1 h) \end{bmatrix} \begin{bmatrix} 1 \\ -\frac{p_2}{n_2^2} \end{bmatrix} = 0, \quad (2.44)$$

and the equivalent phase-type dispersion equation by solving Eq. (2.44) is as follows:

$$\tan(\kappa_1 h) = \frac{n_1^2 \kappa_1 (n_2^2 p_0 + n_0^2 p_2)}{n_0^2 n_2^2 \kappa_1^2 - n_1^4 p_0 p_2}. \quad (2.45)$$

2.3 WKB Approximation [3, 4]

Before we embark on the bound states of the graded-index optical waveguide, we first review briefly the widely applied WKB approximation, which has also found wide application in optical waveguide theory. Let us begin with the mathematical derivation of the WKB wave function, and consider again the solutions of the scalar wave equation:

$$\frac{d^2 \psi(x)}{dx^2} + (k^2 n^2(x) - \beta^2) \psi(x) = 0. \quad (2.46)$$

If we suppose the potential varies very slowly, then we can write the trial solution as a combination of two plane waves traveling leftward and rightward, respectively:

$$\psi(x) = A(0) \exp(ikS(x)) + B(0) \exp(-ikS(x)), \quad (2.47)$$

which is a good approximation only when the refractive index varies very slowly. How slow? For simplicity, inserting a rightward traveling plane wave into the wave equation, one will get a differential equation of $S(x)$:

$$\left(\frac{dS}{dx} \right)^2 + \frac{1}{ik} \frac{d^2 S}{dx^2} = n^2(x) - \frac{\beta^2}{k^2}. \quad (2.48)$$

We now expand $S(x)$ in the power series in $1/k$ and write as follows:

$$S = S_0 + \frac{1}{k} S_1 + \left(\frac{1}{k} \right)^2 S_2 + \dots. \quad (2.49)$$

Feeding this into Eq. (2.48) and requiring that all terms of $O(\hbar^n)$ vanish independently, there is

$$\left| \frac{d\lambda}{dx} \right| \ll 1. \quad (2.50)$$

where

$$\lambda = \frac{2\pi}{\sqrt{k^2 n(x)^2 - \beta^2}}. \quad (2.51)$$

Equation (2.50) requires that the refractive index should vary slowly, and there is

$$\left| \frac{n(x)\lambda}{2\pi(n(x)^2 - \beta^2/k^2)} \frac{dn(x)}{dx} \right| \ll 1. \quad (2.52)$$

If Eq. (2.52) is satisfied, and we ignore all terms of $O(1/k^n) (n \geq 2)$ in Eq. (3.4), we can rewrite down S_0 , S_1 as follows:

$$\begin{cases} S_0 = \frac{1}{k} \int (k^2 n(x)^2 - \beta^2)^{1/2} dx \\ S_1 = \frac{i}{2} \ln \left| \frac{dS_0}{dx} \right| \end{cases}, \quad (2.53)$$

and the first-order WKB wave function Eq. (2.47) as follows:

$$\begin{cases} \psi(x) = \frac{A}{\sqrt{\kappa}} \exp[i \int^x \kappa dx] + \frac{B}{\sqrt{\kappa}} \exp[-i \int^x \kappa dx] & \kappa^2 = k^2 n^2(x) - \beta^2 > 0 \\ \psi(x) = \frac{A}{\sqrt{p}} \exp[i \int^x p dx] + \frac{B}{\sqrt{p}} \exp[-i \int^x p dx] & p^2 = \beta^2 - k^2 n^2(x) > 0 \end{cases} \quad (2.54)$$

Equation (2.54) shows that we should anticipate an oscillatory behavior in a region where $k^2 n^2(x) > \beta^2$ and an evanescent behavior in the opposite region. In the region of turning point given by $kn(x) = \beta$, the WKB wave function breaks down since Eq. (2.52) is no longer fulfilled. In order to construct a globally WKB wave function, connection formulas at turning points are required to match to the WKB solutions on both sides of the turning point regions, where the local wavelength λ is singular. Here, we present the connection formulas directly, and the mathematics progresses are referred to the related references. Suppose the position of the turning point is given by x_t , and let us identify the region $k^2 n^2(x) > \beta^2$ with $x < x_t$ and vice versa. The corresponding connecting formula is as follows:

$$\frac{1}{2\sqrt{p}} \exp\left(-\frac{1}{\hbar} \int_{x_t}^x p(x) dx\right) \leftrightarrow \frac{1}{\sqrt{\kappa}} \cos\left(\frac{1}{\hbar} \int_x^{x_t} p(x) dx - \frac{\pi}{4}\right) \quad (2.55)$$

$$(k^2 n^2(x) < \beta^2) \quad (k^2 n^2(x) > \beta^2).$$

However, in some issues that the wave function in the optically dense media is not the superposition of two waves propagate in the opposite directions, such as the transmitted waves left the optically sparse media and traveled to infinite, the connection formula should be replaced by

$$\frac{1}{\sqrt{p}} \exp\left(\int_x^{x_l} p(x) dx\right) \leftrightarrow -\frac{1}{\sqrt{\kappa}} \exp\left(i \int_{x_l}^x \kappa dx + \frac{i\pi}{4}\right) \quad (2.56)$$

$$(k^2 n^2(x) < \beta^2) \quad (k^2 n^2(x) > \beta^2).$$

Instead of the two conventional expressions above, Prof. Friedrich [5] proposed that the application of the WKB approximation can be significantly extended if the connection formulas in the most general case can be used. These expressions can be written as follows:

$$\frac{2}{\sqrt{p(x)}} \cos\left(\int_{x_l}^x p(x) dx - \frac{\phi}{2}\right) \leftrightarrow \frac{N}{\sqrt{p}} \exp\left(-\int_x^{x_l} p dx\right), \quad (2.57)$$

$$\frac{1}{\sqrt{\kappa}} \cos\left(\int_x^{x_l} \kappa dx - \frac{\bar{\phi}}{2}\right) \leftrightarrow \frac{\bar{N}}{\sqrt{p}} \exp\left(\int_{x_l}^x p(x) dx\right). \quad (2.58)$$

There are four parameters N, \bar{N}, ϕ , and $\bar{\phi}$ to be determined by considering the specific problems. And the conventional formulas can be retrieved by setting $N = 1$ and $\phi = \pi/2$. If we consider a superposition of the above two expressions $\psi = A \times (3.39) + B \times (3.40)$ with arbitrary complex coefficients A and B , the conservation condition of the current density on the two sides of the turning point requires that

$$N\bar{N} = \sin\left(\frac{\phi - \bar{\phi}}{2}\right), \quad (2.59)$$

which can be used to determine the undetermined parameters. Imagine a refractive index profile that varies slowly, where the two turning points x_{tl} and x_{tr} are defined via $n(x_{tl}) = n(x_{tr}) = \beta/\kappa$, so there will be oscillatory behavior in the region $x_{tl} < x < x_{tr}$ and evanescent behavior elsewhere. The WKB waves in the region $x_{tl} < x < x_{tr}$ can be defined as follows:

$$\psi_{WKB}(x) \propto \frac{1}{\sqrt{\kappa(x)}} \cos\left(\int_{x_{tl}}^x \kappa(x') dx' - \frac{\phi_l}{2}\right), \quad (2.60)$$

from the left turning point, or equivalently

$$\psi_{WKB}(x) \propto \frac{1}{\sqrt{\kappa(x)}} \cos \left(\int_x^{x_r} \kappa(x') dx' - \frac{\phi_r}{2} \right), \quad (2.61)$$

from the right turning point. ϕ_l and ϕ_r are the reflection phases at the left and right turning points, respectively, and x is an arbitrary point in the well away from the turning points. According to connection expression (2.55), we have $\phi_l = \phi_r = \pi/2$ here. So the two expressions above must agree with each other, and this requirement can only be satisfied when the sum of the two arguments equals an integral multiple of π , which yields the following:

$$\int_{x_l}^{x_r} \kappa(x) dx = \left(n + \frac{1}{2}\right)\pi, \quad (2.62)$$

where $n = 0, 1, 2, \dots$. The above expression is the famous WKB resonance condition and may be used to find the eigenvalue equation for a graded-index waveguide with n as the mode number. The above formula is valid, provided that the two turning points are positioned sufficiently far apart.

In conclusion, in this section, we review briefly the semiclassical WKB approximation, including its wave function and the eigenvalue equation (quantization condition). And it should be noted that the basic WKB wave function ignores all terms of $O(1/k^n)$ ($n \geq 2$), and the phase shift ϕ_l, ϕ_r at the turning points in the original WKB approximation is equal to $\pi/2$.

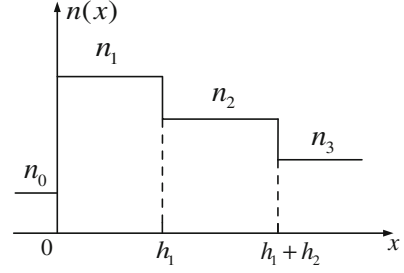
2.4 Multilayer Optical Waveguides

2.4.1 Asymmetric Four-Layer Slab Waveguide [6]

In the beginning of this section, we use a simple asymmetric slab waveguide to demonstrate the existence of the scattered subwaves, which can be simply defined as follows: All the waves being reflected at non-classical turning points for at least once are referred as the scattered subwaves. In contrast, the waves that only reflected at classical turning points are called as the main waves. This is the first time we proposed the concept of the scattered subwaves in this book. Like many other basic concepts, the seemingly simple concept of scattered subwaves is not as straightforward as one might assume.

We are now in a position to deal with the four-layer dielectric slab waveguide via the transfer matrix method. As plotted in Fig. 2.3, two uniform isotropic dielectric of refractive indexes n_1 and n_2 and thicknesses h_1 and h_2 , are sandwiched between two semi-infinite layers of lower index n_0 and n_3 . For definiteness,

Fig. 2.3 The refractive index distribution of a four-layer dielectric slab waveguide



considering the situation $n_1 > n_2 > n_3 > n_0$, which yields an asymmetric guiding structure, and we are interested in those guide modes, whose power is confined largely to the central layer of the guide. So in this chapter, we only consider two cases for the propagation constant β , including (A) $kn_2 \geq \beta \geq kn_3$, that both regions 1 and 2 are the regions of electromagnetic confinement; (B) $kn_1 \geq \beta \geq kn_2$, that only region 1 is the primary region of energy confinement. The discussion on the case of leaky waves is left to the fourth chapter.

For case A of $kn_2 \geq \beta \geq kn_3$, the eigenvalue equation of the matrix form can be immediately written as follows:

$$[-p_0 \quad 1]M_1M_2 \begin{bmatrix} 1 \\ -p_3 \end{bmatrix} = 0, \quad (2.63)$$

where

$$M_1 = \begin{bmatrix} \cos(\kappa_1 h_1) & -\frac{1}{\kappa_1} \sin(\kappa_1 h_1) \\ \kappa_1 \sin(\kappa_1 h_1) & \cos(\kappa_1 h_1) \end{bmatrix}, \quad (2.64)$$

$$M_2 = \begin{bmatrix} \cos(\kappa_2 h_2) & -\frac{1}{\kappa_2} \sin(\kappa_2 h_2) \\ \kappa_2 \sin(\kappa_2 h_2) & \cos(\kappa_2 h_2) \end{bmatrix}, \quad (2.65)$$

$$\left. \begin{aligned} \kappa_1 &= (k_0^2 n_1^2 - \beta^2)^{1/2} \\ \kappa_2 &= (k_0^2 n_2^2 - \beta^2)^{1/2} \\ p_0 &= (\beta^2 - k_0^2 n_0^2)^{1/2} \\ p_3 &= (\beta^2 - k_0^2 n_3^2)^{1/2} \end{aligned} \right\}. \quad (2.66)$$

Substituting the matrixes into Eq. (2.63), the eigenvalue equation of the asymmetric four-layer slab waveguide is as follows:

$$\kappa_1 h_1 = m\pi + \tan^{-1} \left(\frac{p_0}{\kappa_1} \right) + \tan^{-1} \left(\frac{p_2}{\kappa_1} \right), \quad (m = 0, 1, 2, \dots), \quad (2.67)$$

where

$$p_2 = \kappa_2 \tan \left[\tan^{-1} \left(\frac{p_3}{\kappa_2} \right) - \kappa_2 h_2 \right]. \quad (2.68)$$

In order to see the physical insight of the above expression, we define a new quantity Φ_2 , which is given by the following:

$$\Phi_2 = \tan^{-1} \left(\frac{p_2}{\kappa_2} \right), \quad (2.69)$$

and which can be rewritten in the following form according to Eq. (2.68):

$$\kappa_2 h_2 + \Phi_2 = m' \pi + \tan^{-1} \left(\frac{p_3}{\kappa_2} \right), \quad (m' = 0, 1, 2, \dots). \quad (2.70)$$

Combine Eqs. (2.69) and (2.70) with the equation below:

$$\tan^{-1} \left(\frac{p_2}{\kappa_1} \right) = \tan^{-1} \left[\frac{\kappa_2}{\kappa_1} \tan(\Phi_2) \right]. \quad (2.71)$$

We finally obtain an eigenvalue equation that has a similar form of the three-layer slab waveguide

$$\kappa_1 h_1 + \kappa_2 h_2 + \Phi(s) = m \pi + \tan^{-1} \left(\frac{p_0}{\kappa_1} \right) + \tan^{-1} \left(\frac{p_3}{\kappa_2} \right), \quad (2.72)$$

$$(m = 0, 1, 2, \dots)$$

where

$$\Phi(s) = \Phi_2 - \tan^{-1} \left(\frac{\kappa_2}{\kappa_1} \tan \Phi_2 \right). \quad (2.73)$$

To clarify the physics behind the unknown $\Phi(s)$, let us consider the special case of $\frac{n_1^2 - n_2^2}{n_1^2} \ll 1$, which follows that $\frac{\kappa_1 - \kappa_2}{\kappa_1} \ll 1$. Using differential formula, there is

$$\begin{aligned} \tan^{-1} \left(\frac{\kappa_2}{\kappa_1} \tan \Phi_2 \right) &= \tan^{-1} \left[\left(1 - \frac{\kappa_1 - \kappa_2}{\kappa_1} \right) \tan \Phi_2 \right] \\ &\approx \Phi_2 - \frac{\kappa_1 - \kappa_2}{2\kappa_1} \sin 2\Phi_2, \end{aligned} \quad (2.74)$$

and according to Eq. (2.73), one can obtain

$$\Phi(s) = \frac{\kappa_1 - \kappa_2}{2\kappa_1} \sin 2\Phi_2. \quad (2.75)$$

The amplitude of the right-hand side of Eq. (2.75) under first-order approximation is as follows:

$$\frac{\kappa_1 - \kappa_2}{2\kappa_1} \approx \frac{\kappa_1 - \kappa_2}{\kappa_1 + \kappa_2}, \quad (2.76)$$

which denotes the reflection coefficient of light incident from region 1 to region 2. Consequently, $\Phi(s)$ can be viewed as the reflection phase contribution of the first-order scattered subwaves. Of course, the term $\Phi(s)$ denotes the phase contribution of all the scattered subwaves if we did not carry out any approximation. On the contrary, if $n_1 = n_2$ holds, there is $\Phi(s) = 0$. As a summary, $\Phi(s)$ is the phase contribution induced by the reflection occurs at the interface between regions 1 and 2, and is determined by the difference of the refractive index between the two regions. So when dealing with multilayer waveguide, both phase contribution of the main waves and the scattered subwaves should be taken into consideration.

For case B $k_0 n_1 > \beta > k_0 n_2$, whose guiding layer locates in the region of $(0, h_1)$. In this case, the matrix form of the eigenvalue equation can still be written as Eq. (2.63), but the κ_2 in Eq. (2.65) should be modified as follows:

$$\kappa_2 = i(\beta^2 - k_0^2 n_2^2)^{1/2} = i\alpha_2. \quad (2.77)$$

Consequently, the sine and cos in the matrix should be replaced as sinh and cosh, that is,

$$\sin(\kappa_2 h_2) = i \sinh(\alpha_2 h_2), \quad \cos(\kappa_2 h_2) = \cosh(\alpha_2 h_2). \quad (2.78)$$

And the transfer matrix M_2 becomes

$$M_2 = \begin{bmatrix} \cosh(\alpha_2 h_2) & -\frac{1}{\alpha_2} \sinh(\alpha_2 h_2) \\ -\alpha_2 \sinh(\alpha_2 h_2) & \cosh(\alpha_2 h_2) \end{bmatrix}. \quad (2.79)$$

So the eigenvalue equation for this case is mathematically the same with Eq. (2.67), except that p_2 is defined by

$$p_2 = \alpha_2 \tanh \left[\tanh^{-1} \left(\frac{p_3}{\alpha_2} \right) + \alpha_2 h_2 \right]. \quad (2.80)$$

To see the scattered subwaves in the four-layer slab waveguide in another way, let us reconsider the case A for TE mode, whose transverse electric field may be expressed as follows:

$$E_y(x) = \begin{cases} A_0 \exp(p_0 x) & -\infty < x < 0 \\ A_1 \exp(i\kappa_1 x) + B_1 \exp(-i\kappa_1 x) & 0 < x < h_1 \\ A_2 \exp[i\kappa_2(x - h_1)] + B_2 \exp[-i\kappa_2(x - h_1)] & h_1 < x < h_1 + h_2 \\ A_3 \exp[-p_3(x - h_1 - h_2)] & h_1 + h_2 < x < +\infty \end{cases} \quad (2.81)$$

where

$$\left. \begin{aligned} \kappa_1 &= (k_0^2 n_1^2 - \beta^2)^{1/2} \\ \kappa_2 &= (k_0^2 n_2^2 - \beta^2)^{1/2} \\ p_0 &= (\beta^2 - k_0^2 n_0^2)^{1/2} \\ p_3 &= (\beta^2 - k_0^2 n_3^2)^{1/2} \end{aligned} \right\}.$$

Using the continuity condition of E_y and $\partial E_y / \partial x$ at boundaries $x = 0$, $x = h_1$, and $x = h_1 + h_2$, one may write down the dispersion equation as follows:

$$\begin{aligned} \exp[i2(\kappa_1 h_1 + \kappa_2 h_2 - \Phi_{10} - \Phi_{23})] + \frac{\kappa_1 - \kappa_2}{\kappa_1 + \kappa_2} \exp[i2(\kappa_1 h_1 - \Phi_{10})] \\ + \frac{\kappa_2 - \kappa_1}{\kappa_2 + \kappa_1} \exp[i2(\kappa_2 h_2 - \Phi_{23})] = 1, \end{aligned} \quad (2.82)$$

where

$$\Phi_{10} = \tan^{-1} \left(\frac{p_0}{\kappa_1} \right) \quad (2.83)$$

$$\Phi_{23} = \tan^{-1} \left(\frac{p_3}{\kappa_2} \right) \quad (2.84)$$

What does Eq. (2.82) means? See Fig. 2.4 for the zigzag path of rays in the slab waveguide. Clearly, the first term on the left-hand side of Eq. (2.82) denotes the main waves which are plotted with solid lines in Fig. 2.4. Starting from the interface between regions 0 and 1, the main waves travels through the interface between regions 1 and 2 and then is total-reflected at the boundary of region 3. In summary, the main waves only is total-reflected at the boundaries of regions 0 and 3. On the contrary, the dotted lines shown in Fig. 2.4 represent the second and third terms in Eq. (2.82), which are reflected at the interface between regions 1 and 2. So these two terms denote the scattered subwaves. The guided modes in the slab waveguide are in fact the coherent superposition result of the main waves and the scattered subwaves, which are ignored in the semiclassical theories. It can be proved mathematically that Eq. (2.82) can be recast as follows:

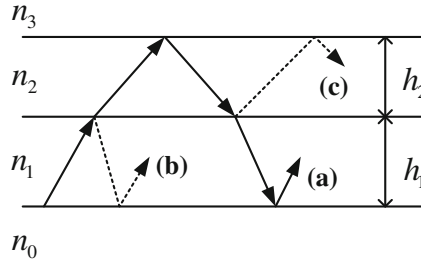


Fig. 2.4 Zigzag path of the main waves (a) and the scattered subwaves (b, c) in the four-layer dielectric waveguide

$$\exp\{i2[\kappa_1 h_1 + \kappa_2 h_2 + \Phi(s) - \Phi_{10} - \Phi_{23}]\} = 1. \quad (2.85)$$

In view of $\exp(i2m\pi) = 1$, ($m = 0, 1, 2, \dots$), the above equation is equivalent with Eq. (2.72).

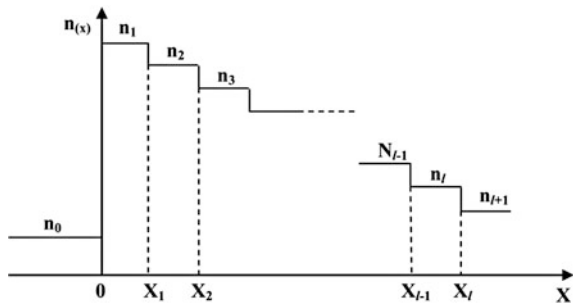
2.4.2 Multilayer Slab Waveguide

In this section, we expand the conclusions of the four-layer slab waveguide to the multilayer slab waveguide. Suppose there are l layers of index n_1, n_2, \dots, n_l , and thickness of h_1, h_2, \dots, h_l , embedded in two cladding layers of index n_0 and n_{l+1} . For the structure consider here, there is $n_1 > n_2 > \dots > n_l > n_{l+1} > n_0$ (Fig. 2.5).

Let us extend Eq. (2.63) to this waveguide structure, consider the guided modes with $kn_l > \beta > kn_{l+1}$, and the eigenvalue equation for the TE mode in the matrix form can be written as follows:

$$\begin{bmatrix} -p_0 & 1 \end{bmatrix} \prod_{i=1}^l M_i \begin{bmatrix} 1 \\ -p_{l+1} \end{bmatrix} = 0, \quad (2.86)$$

Fig. 2.5 Asymmetric $l + 2$ layer slab waveguide



where the matrix corresponding to the i th layer M_i has the following form:

$$M_i = \begin{bmatrix} \cos(\kappa_i h_i) & -\frac{1}{\kappa_i} \sin(\kappa_i h_i) \\ \kappa_i \sin(\kappa_i h_i) & \cos(\kappa_i h_i) \end{bmatrix} \quad (2.87)$$

where

$$\begin{cases} \kappa_i = (k_0^2 n_i^2 - \beta^2)^{1/2} \\ p_0 = (\beta^2 - k_0^2 n_0^2)^{1/2} \\ p_{l+1} = (\beta^2 - k_0^2 n_{l+1}^2)^{1/2} \end{cases}.$$

Equation (2.86) can be simplified via direct algebraic manipulations as

$$\kappa_1 h_1 = m\pi + \tan^{-1}\left(\frac{p_0}{\kappa_1}\right) + \tan^{-1}\left(\frac{p_2}{\kappa_1}\right), \quad (2.88)$$

$(m = 0, 1, 2, \dots)$

where

$$p_i = \kappa_i \tan \left[\tan^{-1}\left(\frac{p_{i+1}}{\kappa_i}\right) - \kappa_i h_i \right] \quad (2.89)$$

$i = (2, 3, \dots, l)$

The two formula above completely specify the dispersion characteristics of the asymmetric multilayer slab waveguide. However, Eq. (2.89) is a recurrence formula, which requires all the information of $p_j (j > i)$ to calculate p_i . To see the different roles of the main waves and the scattered subwaves, we define

$$\phi_i = \tan^{-1}\left(\frac{p_i}{\kappa_i}\right), \quad (2.90)$$

According to Eq. (2.89), one obtains

$$\begin{aligned} \phi_i &= m_i \pi + \tan^{-1}\left(\frac{p_{i+1}}{\kappa_i}\right) - \kappa_i h_i \\ &= m_i \pi + \tan^{-1}\left(\frac{\kappa_{i+1}}{\kappa_i} \tan \phi_{i+1}\right) - \kappa_i h_i \\ &\quad (m_i = 0, 1, 2, \dots; i = 1, 2, \dots, l-1), \end{aligned} \quad (2.91)$$

which can be modified as

$$\kappa_i h_i + \left[\phi_{i+1} - \tan^{-1}\left(\frac{\kappa_{i+1}}{\kappa_i} \tan \phi_{i+1}\right) \right] = m_i \pi + (\phi_{i+1} - \phi_i). \quad (2.92)$$

$(m_i = 0, 1, 2, \dots; i = 1, 2, \dots, l-1)$

When $i = l$, there is

$$\kappa_l h_l = m_l \pi + \tan^{-1} \left(\frac{p_{l+1}}{\kappa_l} \right) - \phi_l, \quad (2.93)$$

Based on the three equations above and sum up over i , one can write down

$$\begin{aligned} \sum_{i=1}^l \kappa_i h_i + \sum_{i=1}^{l-1} \left[\phi_{i+1} - \tan^{-1} \left(\frac{\kappa_{i+1}}{\kappa_i} \tan \phi_{i+1} \right) \right] \\ = m \pi + \tan^{-1} \left(\frac{p_{l+1}}{\kappa_l} \right) - \phi_l. \end{aligned} \quad (2.94)$$

On the other hand, it is easy to prove

$$\phi_1 = m_1 \pi + \tan^{-1} \left(\frac{p_2}{\kappa_1} \right) - \kappa_1 h_1, \quad (2.95)$$

which can be rewritten by inserting Eq. (2.88)

$$\phi_1 = m_1 \pi - \tan^{-1} \left(\frac{p_0}{\kappa_1} \right). \quad (2.96)$$

Finally, we transformed Eq. (2.94) into

$$\begin{aligned} \sum_{i=1}^l \kappa_i h_i + \Phi(s) = m \pi + \tan^{-1} \left(\frac{p_0}{\kappa_1} \right) + \tan^{-1} \left(\frac{p_{l+1}}{\kappa_l} \right), \\ (m = 0, 1, 2, \dots) \end{aligned} \quad (2.97)$$

with the phase contribution of the scattered subwaves

$$\Phi(s) = \sum_{i=1}^{l-1} \left[\phi_{i+1} - \tan^{-1} \left(\frac{\kappa_{i+1}}{\kappa_i} \tan \phi_{i+1} \right) \right]. \quad (2.98)$$

We can obtain the eigenvalue equation of the three-layer or four-layer slab structure from Eq. (2.97) by setting $l = 1$, or $l = 2$, respectively. It is obvious that this formula can be applied to any multilayer structures without any approximation. Furthermore, it has a clear physical explanation that both the main waves and scattered subwaves contribute to the total phase contribution. Although the discussion above consider only the case of $\beta < k_0 n_i$, it is not difficult to obtain the corresponding result related to the case of $\beta > k_0 n_i$, by just replacing the κ_j with $i\alpha_j$ in the matrix M_j for all the $j > i$. Interesting readers can also derive the eigenvalue equation for TM modes by using the appropriate matrix.

2.5 The Transfer Matrix Treatment of the Graded-Index Waveguide

2.5.1 The Eigenvalue Equation

In this section, the transfer matrix method is extended to treat the graded-index waveguide, and it is demonstrated strictly that the phase shifts at the turning points are exact equal to π . Since this section deals with the general graded-index structure with arbitrary refractive index profile, the strategy is as follows: We first approximate the graded-index waveguide with a multilayer waveguide with n layers and then take the limit as the n approaches infinite. At the beginning, let us consider a simple case in which only one turning point exists (Fig. 2.6).

Assume that the turning point locates at the position $x = x_t$, and the index profile extends to infinite. In order to apply the transfer matrix method, we should truncate infinite at $x_s = x_t + x_c$ for sufficient large x_c , and set $n(x) = n_s$ for $x > x_s$. Then, the regions $(0, x_t)$ and (x_t, x_s) are divided into l and m segments, with each layer has the same thickness h , so that $x_t = lh$ and $x_c = mh$. For TE mode, the transfer matrix for these segments is as follows:

$$M_i = \begin{bmatrix} \cos(\kappa_i h) & -\frac{1}{\kappa_i} \sin(\kappa_i h) \\ \kappa_i \sin(\kappa_i h) & \cos(\kappa_i h) \end{bmatrix} \quad (i = 1, 2, \dots, l), \quad (2.99)$$

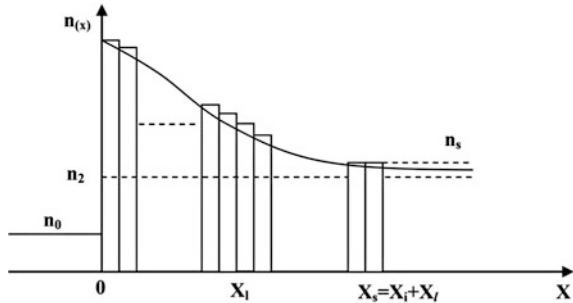
and

$$M_j = \begin{bmatrix} \cosh(\alpha_j h) & -\frac{1}{\alpha_j} \sinh(\alpha_j h) \\ -\alpha_j \sinh(\alpha_j h) & \cosh(\alpha_j h) \end{bmatrix} \quad (j = l+1, l+2, \dots, l+m), \quad (2.100)$$

where

$$\begin{aligned} \kappa_i &= [k_0^2 n^2(x_i) - \beta^2]^{1/2} \\ \alpha_j &= [\beta^2 - k_0^2 n^2(x_j)]^{1/2}. \end{aligned} \quad (2.101)$$

Fig. 2.6 Graded-index structure with only one turning point



According to the transfer matrix method, the corresponding matrix equation is as follows:

$$\begin{bmatrix} E_y(0) \\ E'_y(0) \end{bmatrix} = \left[\prod_{i=1}^l M_i \right] \left[\prod_{j=l+1}^{l+m} M_j \right] \begin{bmatrix} E_y(x_s) \\ E'_y(x_s) \end{bmatrix}, \quad (2.102)$$

while the evanescent behavior in both the outer claddings in the approximated multilayer structure are given by

$$E_y(x) = \begin{cases} A_0 \exp(p_0 x) & (x < 0) \\ A_s \exp[-p_s(x - x_s)] & (x > x_s) \end{cases}, \quad (2.103)$$

where

$$\begin{aligned} p_0 &= (\beta^2 - k_0^2 n_0^2)^{1/2} \\ p_s &= (\beta^2 - k_0^2 n_s^2)^{1/2}. \end{aligned} \quad (2.104)$$

Substituting Eq. (2.103) into Eq. (2.102), we have

$$\begin{pmatrix} -p_0 & 1 \end{pmatrix} \left(\prod_{i=1}^l M_i \right) \left(\prod_{j=l+1}^{l+m} M_j \right) \begin{pmatrix} 1 \\ -p_s \end{pmatrix} = 0. \quad (2.105)$$

By a simple algebraic process, the above formula can be recast into

$$\begin{pmatrix} -p_0 & 1 \end{pmatrix} \left(\prod_{i=1}^l M_i \right) \begin{pmatrix} 1 \\ -p_{l+1} \end{pmatrix} = 0, \quad (2.106)$$

where

$$\begin{cases} p_j = \alpha_j \frac{\sinh(\alpha_j h) + \frac{p_{l+1}}{\alpha_j} \cosh(\alpha_j h)}{\cosh(\alpha_j h) + \frac{p_{l+1}}{\alpha_j} \sinh(\alpha_j h)} \\ (j = l+1, l+2, \dots, l+m) \\ p_{l+m+1} = p_s \end{cases} \quad (2.107)$$

So it is clear that in Eq. (2.106), the field distribution outside the turning point is treated as a exponentially decaying field, that is,

$$E_y(x) = A_t \exp[-p_{l+1}(x - x_t)] \quad (x > x_t). \quad (2.108)$$

Similar with the process we used in the last section, the exact eigenvalue equation can be derived from Eq. (2.106)

$$\sum_{i=1}^l \kappa_i h + \Phi(s) = N\pi + \tan^{-1}\left(\frac{p_0}{\kappa_1}\right) + \tan^{-1}\left(\frac{p_{l+1}}{\kappa_l}\right), \quad (2.109)$$

$(N = 0, 1, 2, \dots)$

where

$$\Phi(s) = \sum_{i=1}^{l-1} \left[\Phi_{i+1} - \tan^{-1}\left(\frac{\kappa_{i+1}}{\kappa_i} \tan \Phi_{i+1}\right) \right], \quad (2.110)$$

$$\Phi_i = \tan^{-1}\left(\frac{p_i}{\kappa_i}\right), \quad (2.111)$$

$$p_i = \kappa_i \tan \left[\tan^{-1}\left(\frac{p_{i+1}}{\kappa_i}\right) - \kappa_i h \right] \quad (i = 1, 2, \dots, l), \quad (2.112)$$

and $\tan^{-1}\left(\frac{p_{l+1}}{\kappa_l}\right)$ denotes the phase shift at the turning point.

Next considering the graded-index structure, i.e., $l \rightarrow \infty, m \rightarrow \infty$, the first term in the left-hand side of Eq. (2.109) becomes integral

$$\sum_{i=1}^l \kappa_i h_i = \int_0^{x_l} \kappa(x) dx, \quad (2.113)$$

and the second term becomes

$$\sum_{i=1}^{l-1} \left[\Phi_{i+1} - \arctan\left(\frac{\kappa_{i+1}}{\kappa_i} \tan \Phi_{i+1}\right) \right] = \int_0^{x_l} \frac{q}{q^2 + \kappa^2} \frac{d\kappa}{dx} dx. \quad (2.114)$$

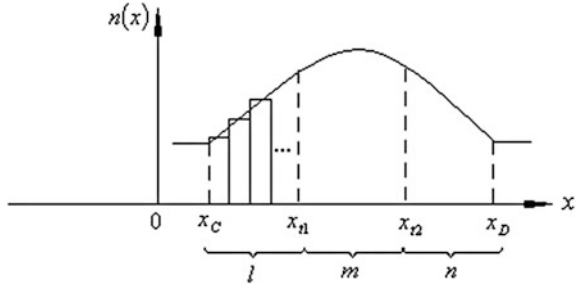
where $q(x) = -E'(x)/E(x)$. Finally, the exact eigenvalue equation of the graded-index slab waveguide can be written as follows:

$$\int_0^{x_l} \kappa dx + \Phi(s) = \int_0^{x_l} \left(\kappa + \frac{q}{q^2 + \kappa^2} \frac{d\kappa}{dx} \right) dx = N\pi + \tan^{-1}\left(\frac{p_0}{\kappa_1}\right) + \tan^{-1}\left(\frac{p_{l+1}}{\kappa_l}\right). \quad (2.115)$$

$(N = 0, 1, 2, \dots)$

It should be note that the term $\Phi(s)$ denotes the phase contribution of the scattered subwaves, and $\frac{q}{q^2 + \kappa^2} \frac{d\kappa}{dx}$ represents its wave number. The above equation can be generalized to the case with two turning points without difficult. Consider the graded-index waveguide with two turning points at x_{t1} and x_{t2} , and extend to infinity on both sides (Fig. 2.7).

Fig. 2.7 A graded-index waveguide with two turning points



Take the similar process used above, first we truncate the index profile $n(x)$ at x_C and x_D , respectively, and divide the regions (x_C, x_{t1}) , (x_{t1}, x_{t2}) , and (x_{t2}, x_D) into l , m , and n segments of the same thickness h . Then, the dispersion equation via the transfer matrix can be written as follows:

$$\int_{x_{t1}}^{x_{t2}} \kappa dx + \Phi(s) = N\pi + \tan^{-1}\left(\frac{p_l}{\kappa_{l+1}}\right) + \tan^{-1}\left(\frac{p_{l+m+1}}{\kappa_{l+m}}\right), \quad (2.116)$$

$(N = 0, 1, 2, \dots)$

where

$$\Phi(s) = \sum_{j=1}^{l+m-1} \left[\Phi_{j+1} - \tan^{-1}\left(\frac{\kappa_{j+1}}{\kappa_j} \tan \Phi_{j+1}\right) \right] \quad (2.117)$$

$$\Phi_j = \tan^{-1}\left(\frac{p_j}{\kappa_j}\right).$$

p_l and p_{l+m+1} are the effective attenuation coefficients for the regions $(x < x_{t1})$ and $(x > x_{t2})$, respectively, which are specified by

$$p_k = \alpha_k \frac{\sinh(\alpha_k h) + \frac{p_{k+1}}{\alpha_k} \cosh(\alpha_k h)}{\cosh(\alpha_k h) + \frac{p_{k+1}}{\alpha_k} \sinh(\alpha_k h)} \quad (2.118)$$

$(k = l + m + 1, l + m + 2, \dots, l + m + n),$

where $p_0 = p_C$ and $p_C = [\beta^2 - k_0^2 n^2(x_C)]^{1/2}$,

$$p_i = \alpha_i \frac{\sinh(\alpha_i h) + \frac{p_{i-1}}{\alpha_i} \cosh(\alpha_i h)}{\cosh(\alpha_i h) + \frac{p_{i-1}}{\alpha_i} \sinh(\alpha_i h)}, \quad (2.119)$$

$(i = 1, 2, \dots, l)$

where $p_{l+m+n+1} = p_D$ and $p_D = [\beta^2 - k_0^2 n^2(x_D)]^{1/2}$.

2.5.2 The Phase Shift at Turning Point [7]

From the last section, it is clear that we can replace the field distribution outside the turning point with an exponentially decaying field without introducing any calculation error. So it is possible to treat the index profile outside the turning point as with a constant n_{eq} , which is smaller than $n(x_t)$ (see Fig. 2.8).

According to the analysis above, the effective attenuation coefficient can be written as follows:

$$p_t = \left(\beta^2 - k_0^2 n_{eq}^2 \right)^{1/2}, \quad (2.120)$$

If we restrict ourselves with the bound electromagnetic modes, p_t must be a finite and positive quantity. Let us prove this statement briefly below.

- (1) For $j = l+m$, consider Eqs. (2.101), (2.104), and (2.107), and there is

$$p_c = p_{l+m+1} > \alpha_{l+m}; \quad (2.121)$$

since both α_j and h are positive real number, it follows

$$\cosh(\alpha_{l+m}h) > \sinh(\alpha_{l+m}h); \quad (2.122)$$

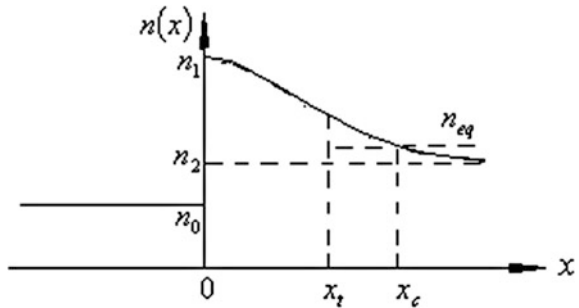
and then, in view of (2.107), one can prove that $p_{l+m} > \alpha_{l+m}$. Repeat the above process, and finally, there is

$$p_{l+1} > \alpha_{l+1}. \quad (2.123)$$

- (2) Let us rewrite Eq. (2.107) into the following formation

$$p_j = p_{j+1} \frac{\cosh(\alpha_j h) + \frac{\alpha_j}{p_{j+1}} \sinh(\alpha_j h)}{\cosh(\alpha_j h) + \frac{p_{j+1}}{\alpha_j} \sinh(\alpha_j h)}. \quad (2.124)$$

Fig. 2.8 Replace the index distribution outside the turning point with an effective refractive index n_{eq}



Obviously, $p_j < p_{j+1}$ holds, which leads to

$$p_l = p_{l+1} < p_{l+m+1} = p_c. \quad (2.125)$$

(3) According to Eqs. (2.123) and (2.125), one obtains

$$\alpha_{l+1} < p_l < p_c, \quad (2.126)$$

which shows that p_l is a finite and real number. However, according to Eq. (2.101), as $l \rightarrow \infty$ ($h \rightarrow 0$), there holds

$$\kappa_l = [k_0^2 n^2(x_l) - \beta^2]^{1/2} \rightarrow [k_0^2 n^2(x_l) - \beta^2]^{1/2} = 0. \quad (2.127)$$

Finally, the phase shift at the turning point can be calculated as follows:

$$\tan^{-1}\left(\frac{p_l}{\kappa_l}\right) = \tan^{-1}\sqrt{\frac{\beta^2 - k_0^2 n_{\text{eq}}^2}{k_0^2 n^2(x_l) - \beta^2}} \rightarrow \frac{\pi}{2} \quad (l \rightarrow \infty), \quad (2.128)$$

which is exact twice the result in the basic WKB approximation. In the modified WKB approximation, the non-integral Maslov index is used, which allows the reflection phase at the turning points approaches $\pi/2$ in the semiclassical limit, and approaches π in the anticlassical limit. Compared with the WKB approximation, the result we derived has the following features:

- (1) The phase shift at the turning point is constant π , which is independent of the propagation constant and the refractive index distribution; it is a general result.
- (2) The phase shift does not related to the position of the turning points, and it does not vary if the turning point is near truncated points, discontinuous points, or other turning points.
- (3) The phase shift is the same for different wavelengths.

Using Eq. (2.128), we can further simplify the eigenvalue equation Eq. (2.115) of an arbitrary graded-index waveguide with only one turning point as plotted in Fig. 2.6 as

$$\int_0^{x_l} \kappa dx + \Phi(s) = m\pi + \tan^{-1}\left(\frac{p_0}{\kappa_1}\right) + \frac{\pi}{2} \quad (m = 0, 1, 2, \dots), \quad (2.129)$$

and the eigenvalue equation of graded-index waveguide with two turning points in Fig. 2.7 as

$$\int_{x_{l1}}^{x_{l2}} \kappa dx + \Phi(s) = (m+1)\pi \quad (m = 0, 1, 2, \dots). \quad (2.130)$$

In conclusion of this section, we started with the transfer matrix and applied to multilayer and graded-index waveguide to obtain an exact and general eigenvalue equation with clear physics. The notion of scattered subwaves, which is completely neglected in semiclassical theories, was proposed and appeared in all the obtained eigenvalue equations.

References

1. M. Born, W. Wolf, Principles of Optics, 6th edn (corrected) (Pergamon Press, Oxford, 1986)
2. A. Yariv, Quantum Electronics, 2nd edn (Wiley, New York 1975)
3. L.I. Schiff, Quantum Mechanics (McGraw-Hill, New York, 1955)
4. A. Gedeon, Comparison between rigorous theory and WKB-analysis of modes in graded-index waveguides. *Opt. Commun.* **12**, 329 (1974)
5. H. Friedrich, J. Trost, Working with WKB waves far from the semiclassical limit. *Phys. Rep.* **397**, 359 (2004)
6. M.J. Sun, M.W. Muller, W.S.C. Chang, Thin-film waveguide gyrators: a theoretical analysis. *Appl. Opt.* **16**, 2986 (1977)
7. Z. Cao, Q. Liu, Y. Jiang, Q. Shen, X. Dou, Y. Ozaki, Phase shift at a turning point in a planar optical waveguide. *J. Opt. Soc. Am. A* **18**, 216 (2001)

Progress in Planar Optical Waveguides

Wang, X.; Yin, C.; Cao, Z.

2016, XI, 241 p. 152 illus., 94 illus. in color., Hardcover

ISBN: 978-3-662-48982-6